Petrology and Geochemistry of the Big Pine Volcanic Field Inyo County, California

By
Ashley Varnell
Geological Sciences Department
California State Polytechnic University
Pomona, CA

Senior Thesis
Submitted in partial fulfillment
of requirements for the
B.S. Geology Degree

Table of Contents

ABSTRACT

The Big Pine volcanic field encompasses 1000 square kilometers of the northern Owens Valley. It is comprised of 30 basaltic cones and flows emplaced over the past 1.2 million years.

In thin section, Big Pine basalts display marked differences. Some samples contain phenocrysts of plagioclase, resorbed olivine and orthopyroxene and minor nepheline. Others have abundant plagioclase and pyroxene phenocrysts, but sparse olivine and no nepheline. There is also a noticeable difference in phenocryst size. Some basalts are comprised of phenocrysts that exceed 1mm in diameter, while others have much smaller (<0.1mm) phenocrysts. There is no apparent relationship between phenocryst size and mineralogy.

Major element analyses support thin section observations. Two distinct groupings are present. One is generally quartz normative (silica-rich), while the second is nepheline normative (silica-poor). Temporal relationships are difficult to establish, but field observations suggest the older flows were more silica undersaturated. Trace element data is enigmatic. There is a subtle trend for the more incompatible elements to favor silica-rich rocks; however, strontium is clearly anomalous.

The bimodal distribution of silica has been well documented for the Cima basalts. There, it is attributed to systematic variation in melting depth over time. A similar explanation for the Big Pine field is difficult to rationalize. Big Pine basalts were emplaced over a shorter time span and display an inverse relationship, characterized by more recent silica-rich basalts. We conclude Big Pine mineralogy and geochemistry are best explained by partial assimilation of Mesozoic granite as basaltic magma rose upward from the underlying mantle.

Introduction

The Big Pine volcanic field is located in the Owens Valley of central California. It is one of several volcanic fields within the Owens Valley and Mojave Desert. Covering an area approximately 1000 square kilometers (Fig. 1), it lies approximately 16 kilometers north of Independence, CA and extends northward for about 22 kilometers. The northern edge of the field lies 2.4 kilometers south of Big Pine. The Big Pine field is one of the most recognizable features within the valley. The flows can be seen along both sides of U.S. 395, stretching from the base of the Sierra Nevada Mountains to the west to the Inyo Mountains to the east.

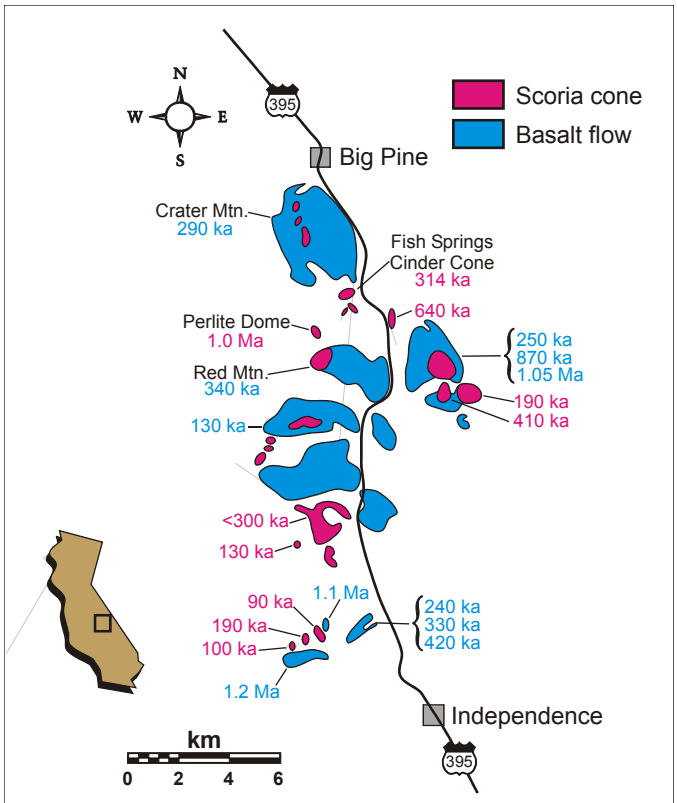

Figure 1. Index Map of Big Pine Volcanic Field showing locations and approximate age.

The Big Pine field is relatively young; the oldest of the flows has been dated at approximately 1.2 Ma, however, most of the flows are younger than 500 ka. Figure 1 shows the location of the Big Pine field as well as the ages of the flows and cones that have been dated. This volcanic field is thought to be a series of magma plumes that rose rapidly from the mantle. The initial eruptions were poor in assimilated crustal rocks; however, subsequent flows display compositional variations due to both differentiation and assimilation of granitic country rock (Bierman et al., 1991)

While the Big Pine volcanic field is the subject of study, a basic understanding of the geology of the Owens Valley and surrounding area is necessary. As you travel north along U.S. 395 the two mountain ranges to your left and right tower above like knights standing guard at the gates of a castle. To your left you will notice the breathtaking Sierra Nevada Mountains. This range of mountains is higher and more jagged in appearance than the gentle giants to the

east. The Inyo-White Mountain range, while not nearly as dramatic, is actually much more geologically complex. Colorful bands comprised of different sedimentary rock units make up a large portion of the Inyo-White Range. The mountain ranges are actually only a part of the story of the Owens Valley. The Owens Valley has one of the most dramatic examples of topographic relief in the United States. There is 10,800 feet of relief between Mount Whitney (14,494 feet) and Lone Pine (3,700 feet) (Sharp and Glazner, 1997).

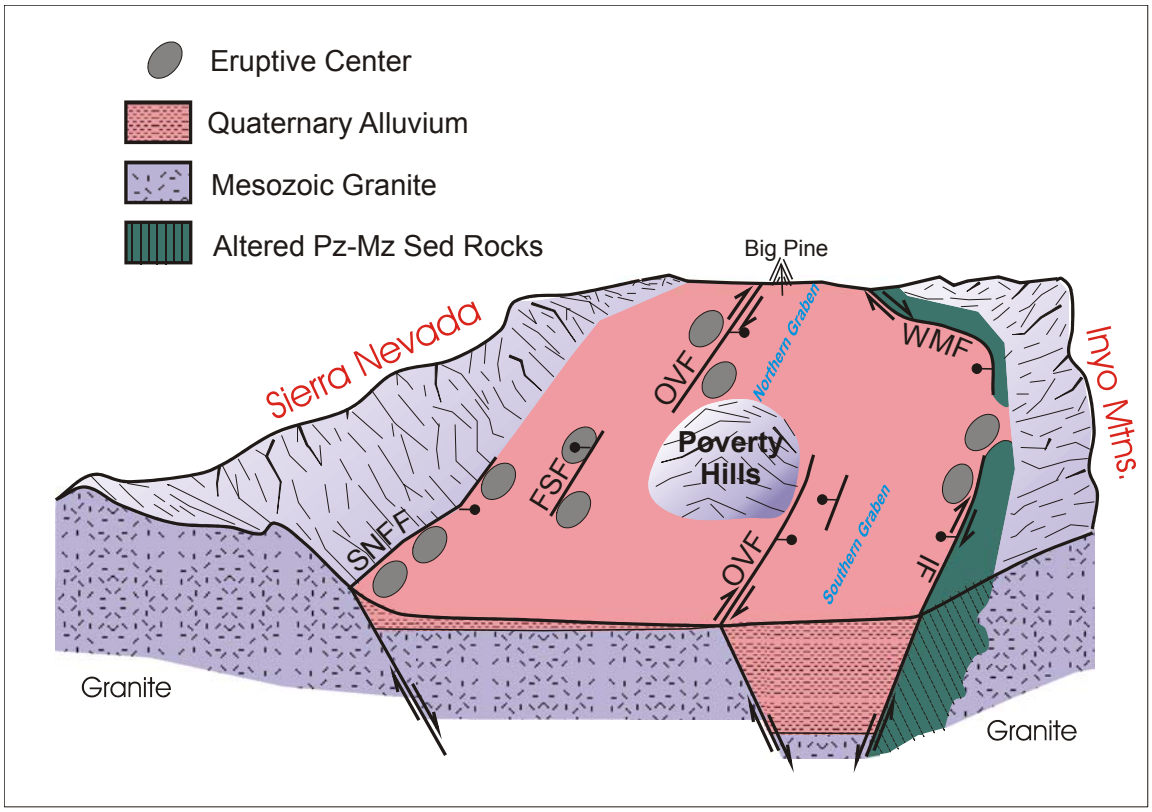

Figure 2. This simplified cross section shows the basaltic cones of the Big Pine Volcanic Field in reference to the two mountain ranges and the two grabens that form the Owens Valley. Cross Section by Jessey, 2006.

The Owens Valley is a northwest-southeast trending basin lying between the Sierra Nevada Mountain Range and the Inyo-White Mountain Range. As shown in cross section (Fig. 2), this valley is comprised of two fault bounded grabens. The northern graben begins south of Bishop and ends just north of the Poverty Hills, approximately 10 kilometers south of Big Pine. The southern graben starts just south of Poverty Hills and continues southward past Lone Pine. Both grabens have been filled with sediment to form two asymmetrical basins. On the western side of the valley the sediment is much thinner than on the eastern side. This asymmetry is a result of greater down-dropping along the Owens Valley fault zone (Bierman et al., 1991).

The sediment in the Owens Valley is very thick. In some areas sediment thickness reaches three kilometers. The area directly surrounding the Big Pine volcanic field is formed by several large alluvial fans that grade eastward into lacustrine sediments. Beneath the sediment filled basin is the faulted basement rock. The basement, like the surrounding mountains, is primarily Cretaceous granodiorite and quartz monzonite.

The formation of the Owens Valley began with the uplift of the Sierra Nevada and Inyo-White Mountain Ranges. The latest uplift began during the northward migration of the Mendocino Triple Junction. The uplift accelerated about 4.5 million years ago, coinciding with increased slip rate along the San Andreas Fault and the rifting of the Gulf of California. During much of the Tertiary, the Sierra Nevada and Inyo-White mountain ranges were uplifting as one. Similar Mesozoic granitic rocks are exposed in both ranges. While these rocks are well exposed in the Sierra Nevada due to erosion, they are still capped with Paleozoic marine sedimentary rocks in the White-Inyo Ranges (Bierman et al., 1991). As these mountains were uplifted, Basin and Range extension began. This extension caused the mountains to split apart by way of normal faults, forming the grabens that underlie the valley floor today.

The Sierra Nevada Mountains are predominantly Cretaceous granodiorite and quartz monzonite. In some locations these rocks become porphyritic while in other areas they are sheared and have a gneissic texture. The roof pendants of the Sierra Nevada are made up of Paleozoic calc-hornfels, marble and biotite schist (Fig. 3).

Although the valley floor is predominately sediment, there is an area in the middle of the Big Pine volcanic field called the Poverty Hills. The Poverty Hills are an uplifted region of bedrock that underlies the valley sediments. These hills are one-third Paleozoic metasediments and two-thirds Mesozoic plutonic rocks. Alternatively, Bishop (2000) has suggested the Poverty Hills represent a mega-avalanche deposit.

The Paleozoic metasediments have been correlated with the marine sedimentary rocks in the Inyo-White Mountain Range to the east. The oldest unit found in the Poverty Hills is the Late Mississippian Rest Spring Shale. The Rest Spring Shale is overlain by the Pennsylvanian Keeler Canyon Formation. These rocks were highly folded prior to the intrusion of the plutonic rocks.

The Mesozoic plutonic rocks found in the Poverty Hills appear to be part of the Tinemaha granodiorite. This granodiorite is medium-grained and equigranular. It is comprised of

quartz, hornblende, biotite and pink, green and gray feldspars. Although the Tinemaha granodiorite has been dated at Middle Jurassic, the granodiorite from the Poverty Hills has not been dated.

On the east side of the Owens Valley are the Inyo-White Mountains. These mountains, while they do have similarities, seem to be more complicated lithologically than the Sierra Nevada Mountains. The lithologic descriptions of the Inyo-White Mountain range are from Donald C. Ross' Independence Quadrangle geologic map (1965).

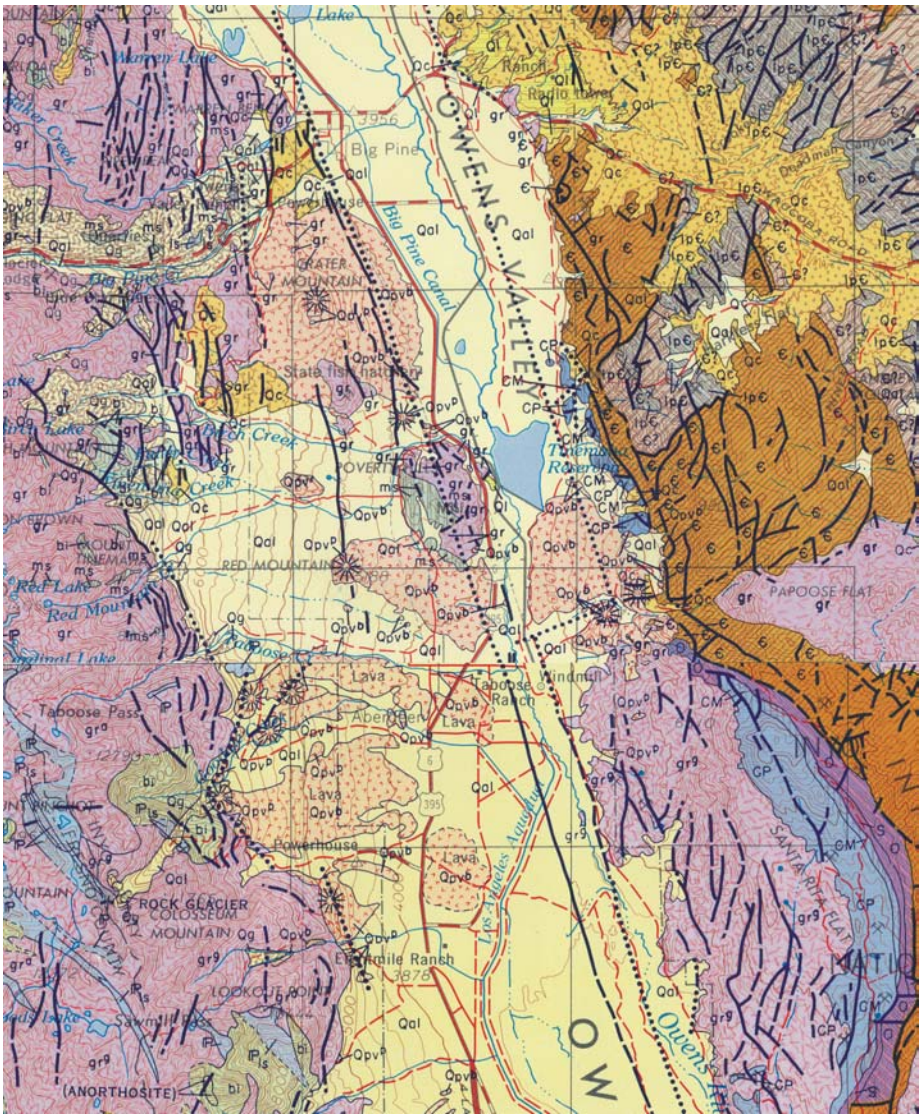

Figure 3. Geologic Map of Big Pine Volcanic Field and surrounding mountains. Adapted from the USGS Fresno and Mariposa maps by Bateman.

The Santa Rita Flat pluton is medium-grained, non-foliated porphyritic quartz monzonite. Around the perimeter of the Santa Rita Flat pluton, small masses and dikes of Cretaceous aplite, alaskite and pegmatite occur. These small masses and dikes are also found in some areas of the Sierra Nevada Mountains. This is further evidence that both mountain ranges began as one mass and were later faulted into two separate mountain ranges.

The youngest sedimentary unit found in the Inyo-White Mountains is the Pennsylvanian to Permian Keeler Canyon Formation. It is approximately 300 meters thick; consisting of thin-bedded, gray limestone and dark-gray shale and siltstone. The Rest Spring Shale lies beneath

the Keeler Canyon. This shale is thought to be Upper Mississippian to Pennsylvanian in age with an average thickness of 800 meters. This unit is commonly metamorphosed to andalusite hornfels.

East of the Rest Spring Shale is the Perdido Formation. This is Mississippian in age and approximately 100 to 200 meters thick. It consists of a mixed clastic sequence of sandstone, conglomerate, calcarenite and shale. Below the Perdido Formation is the Sunday Canyon Formation which is Silurian in age. This formation is described as a graptolitic, limy shale with lesser amounts of limestone.

The Upper to Middle Ordovician Ely Springs Dolomite, Johnson Spring Formation, and Barrel Spring Formation lie below the Sunday Canyon. The Ely Springs Dolomite is from 100 to 200 meters thick, thinning to the north. It is light to dark gray dolomite. The Johnson Spring Formation is a mixed sequence of quartzite, dolomite, and limestone with lesser amounts of siltstone and shale. This formation is from 30 to 120 meters thick. The Barrel Spring Formation averages 30 to 60 meters in thickness. It consists of impure sandstone and limestone overlain by mudstone.

The Badger Flat Limestone, the Al Rose Formation and the Tamarack Canyon Dolomite of the Ordovician age Mazourka Group lie to the north of the field area. The Badger Flat Limestone is a blue-gray, silty limestone, and calcarenite, and a yellowish-gray siltstone. The Al Rose Formation is a brown limestone, shale and mudstone with small amounts of chert. The Tamarack Canyon Dolomite is a gray-weathering, thin-bedded dolomite with black chert nodules. Below the Tamarack Canyon are the Cambrian Lead Gulch Formation and Bonanza King Dolomite. The later comprises many of the more resistant outcrops that form the ridge crest of the Inyo-White Mountains. In general, the sedimentary units dip steeply to the west making the units older as you proceed east to the top of the range.

Many faults can be found in and around the Owens Valley. Some of these had more of an influence on the formation of the Owens Valley than others. The major faults are depicted in Figure 4.

The Inyo Thrust Fault was active prior to the Cenozoic. This fault is responsible for the positioning of Precambrian to Late Ordovician rocks above the Mississippian-Pennsylvanian strata. It was part of a major contractional event along a Triassic tectonic belt stretching from Idaho to southeastern California. The Precambrian to Late Ordovician rocks found in the Inyo-

White Mountains are there as a result of approximately 30 kilometers of eastward displacement and folding. Movement along this fault occurred prior to the Early Jurassic and therefore the Sierra Nevada batholith was not affected. The fault daylights on the eastern side of the Inyo-Whites as the Last Chance Thrust and on the western side of the range just east of the Tinemaha Reservoir.

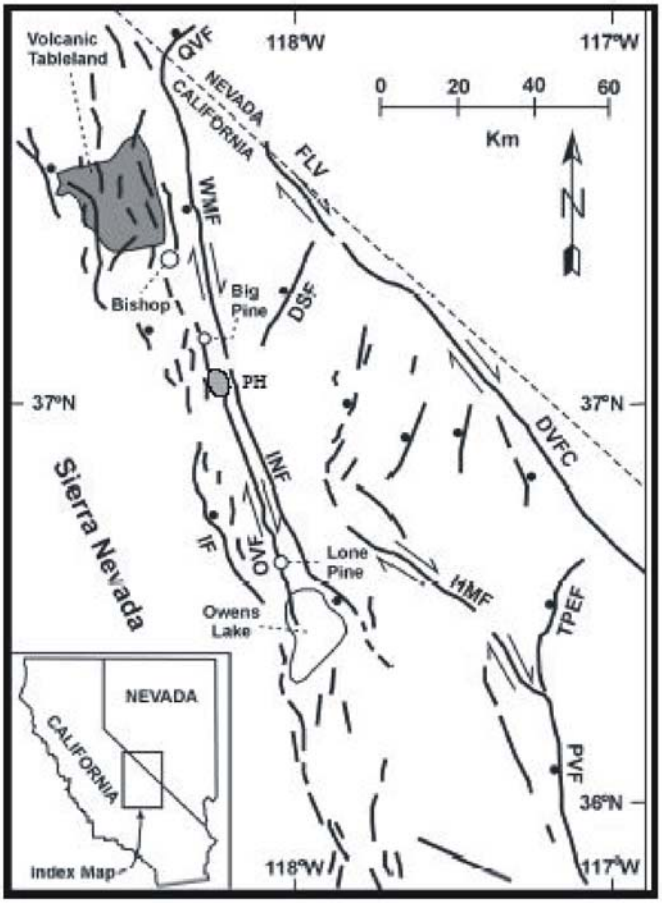

Figure 4. Faults in the Owens Valley; part of the Eastern California Shear Zone. IF- Independence fault; INF- Inyo fault; DVFC- Death Valley-Furnace Creek fault; DSF- Deep Springs fault; OVF- Owens Valley fault; PVF- Panamint Valley fault; QVF- Queen Valley fault; TPEF- Towne Pass- Emigrant fault; WMF- White Mountain fault; HMF- Hunter Mountain fault; FLV- Fish Lake Valley; PH- Poverty Hills (Taylor, 2002).

The Eastern California Shear Zone is a zone of right-lateral shear running north-northwest. This fault zone is responsible for approximately 11 mm/yr of movement between the Sierra Nevada and the Great Basin. The shear zone consists of several fault systems. These are the Death Valley-Furnace Creek, the Hunter Mountain-Panamint Valley, the Fish Lake Valley, and the Owens Valley-White Mountain fault zones.

The Owens Valley Fault is the most important segment of the Eastern California Shear Zone. This fault zone is 120 kilometers long and 3 kilometers wide. It strikes approximately N17°W and is accountable for roughly 1 to 3 mm/yr of right-lateral oblique slip motion (Taylor, 2002; Bierman et al., 1991). The total vertical displacement is less than 2.1 kilometers while the total horizontal displacement is several kilometers. The 1872 Lone Pine earthquake occurred along this fault zone, on a branch called the Lone Pine fault. This earthquake has been estimated to be approximately 7.6 on the moment magnitude and was felt as far away as Oregon and Salt Lake City, Utah (Bierman et al. 1991; Sharp and Glazner, 1997).

One of the other important faults in the Owens Valley is the Independence Fault. This

fault is located at the base of the Sierra Nevada Mountains, the scarps can be seen in the canyons at the base of the mountains, west of the town of Independence. The Independence fault appears to have been responsible for up to half of the subsidence of the Owens Valley. Roughly 1800 meters of offset (east side down) has occurred since the Owens Valley started to form about 6 Ma. The average offset on the Independence Fault is approximately 0.36 mm/yr; however this rate has probably not been constant throughout the life of the fault (Gillespie, 1982).

Previous Works

The Big Pine volcanic field has been studied by numerous researchers. Ross (1965) published a regional geologic map of the northern Owens Valley. He discussed the possibility that some of the flows in the Big Pine field may have originated from faults along the front of the Sierra Nevada Mountains.

Darrow (1972) was the first to complete a comprehensive study of the origin of the Big Pine basalts. His thesis included whole rock geochemistry and minor thin section petrography. Darrow was the first to note that Big Pine basalts were largely alkaline in composition and attributed that alkalinity to the thickened crust beneath the northern Owens Valley. He also noted the anomalous strontium content of Big Pine basalts and concluded that the high strontium values were due to crustal contamination or related to fractionation of early formed magmas.

Gillespie (1982) completed a voluminous and comprehensive study of the geomorphology of the northern Owens Valley. While his research focused mainly on glacial evolution of the landscape, he also compiled and preformed numerous age dates on the Big Pine basalts. He was the major contributing coauthor with Bierman, (Bierman et al., 1991) on a comprehensive paper on the northern Owens Valley. This paper contained several observations not in his original dissertation. Among those were a statement suggesting that the Big Pine field was characterized by bimodal volcanism with earlier basalts more alkaline and later basalts more siliceous. Also, volcanism was thought to have begun about 2 Ma and ceased at about 50,000 years ago.

Waits (1995) studied peridotite inclusions in basalts throughout southern California. While his thesis centered largely on the Cima field, he did analyze a small number of samples from the Big Pine field. He concluded that crustal contamination seems to be limited to non-xenolithic cones. He claims that the non-xenolithic lavas cannot be related to the peridotite bearing lavas by simple fractionation, but may be related through fractionation of olivine and assimilation of crust. It should be noted that the Waits thesis has been the subject of some confusion. He sampled only inclusion-bearing flows and his analyses conclude that the Big Pine basalts are highly alkaline. Later researchers, e.g. (Taylor, 2002), took this as a general statement about the Big Pine field. This, is not the case, his sample population was small and not representative of the overall petrochemistry of the field.

Taylor (2002) completed a Master's thesis on the Poverty Hills that lie near the center of the Big Pine field. While her work centered on structure and the relationships of active faults to

tectonics she did make a few observations regarding the volcanics. She recompiled previous age dates and added newer *He* dates to the database. She also made the statement that Big Pine basalts were highly alkaline, perhaps in reference to the work of Waits. There is no indication she preformed any additional petrology or geochemistry on the basalts.

Blondes (2005) is currently involved with graduate research in the Big Pine field. In a brief abstract she concluded that temporal-compositional trends she observed in a detailed study of a single flow cannot be due to crystal fractionation because the high levels of MgO and Ni limit olivine crystallization to less than 10%, while the *Sr* concentrations would require 40-50%. Blondes also suggests that crustal contamination is unlikely because the basalts contain mantle xenoliths and are primitive; also the SiO_2 and incompatible elements are inversely correlated.

Wang et al. (2002) studied the origin of basalts throughout the southwestern United States. The authors utilized a complex Fe8 index that was based upon whole rocks analyses. It supposedly provides depth of melting. Wang concluded that the depth of melting for the Big Pine basalts is approximately 45-60 kilometers. This agrees nicely with seismic surveys suggesting a crustal thickness of 40-50 kilometers beneath the northern Owens Valley.

Petrography

Plagioclase is the most common phenocrystic phase in Big Pine basalts. Plagioclase is euhedral to subhedral, zoned and occasionally glomerporphyritic. Some phenocrysts show evidence of fracture and breakage, suggesting turbulent transport. Subhedral pyroxene phenocrysts were also present in all thin sections. Both clino and orthopyroxenes were noted; the later often veined and coated by clinopyroxene. Rounding, embayment and resorption was a common feature of some pyroxene grains. Olivine was present in some thin sections and absent in others. Where present, it displayed similar rounding and embayment to that of pyroxene. Some olivine grains occurred as relicts within pyroxene, but most were remarkably unaltered. Small, euhedral, nepheline grains were present in only a few thin sections.

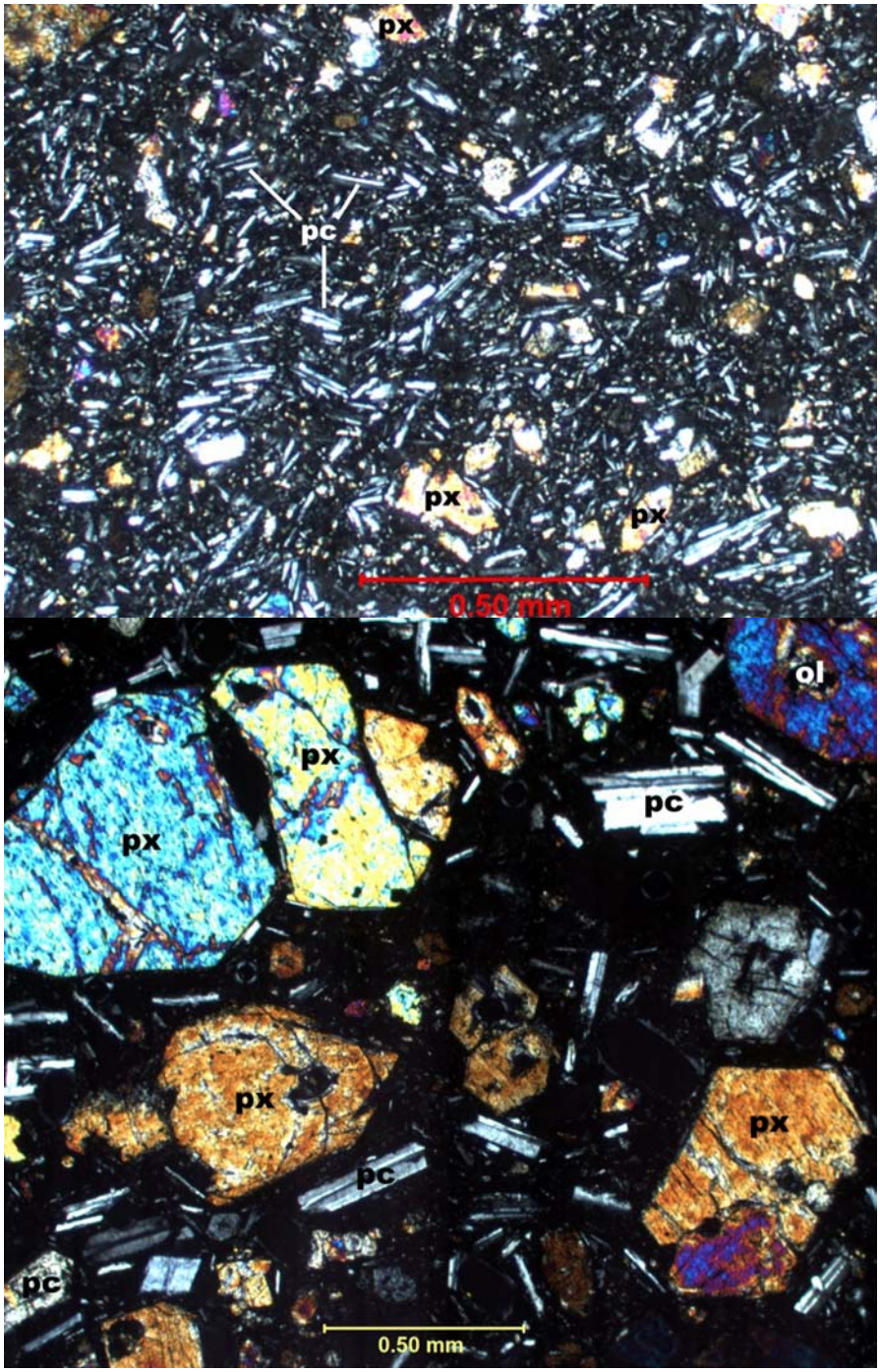

Figure 5a and 5b. Thin sections photomicrographs (crossed nicols) showing the range in phenocryst size. Ol = olivine, px = pyroxene and pc = plagioclase.

The most striking feature in thin section was the significant difference in phenocryst size and percentage (Fig 5a & 5b). Some thin sections contained fewer than five percent phenocrysts, most smaller than 0.1mm; while other thin sections were comprised of >25% phenocrysts often exceeding 1mm in the long dimension. There appears to be little or no relationship between phenocryst size and mineralogy. Furthermore, some researchers have suggested that Big Pine basalt mineralogy shows temporal variation. While the geochemical analyses support this hypothesis, thin sections observations did not. Both of these inconsistencies may be the result of the small number of thin sections prepared for this study. Following is a detailed description of thin sections from individual flows and scoria cones.

Basalts from Crater Mountain had a matrix comprised mainly of plagioclase with some crystals of pyroxene and olivine. The phenocrysts were generally plagioclase, olivine and orthopyroxene. Most of the phenocrysts in the Crater Mountain basalts are greater than 1 mm in the longest dimension. The plagioclase phenocrysts in these samples were occasionally glomeroporphyritic. Much of the olivine in the Crater Mountain flows was altering to pyroxene around the edges and along fractures (Fig 6).

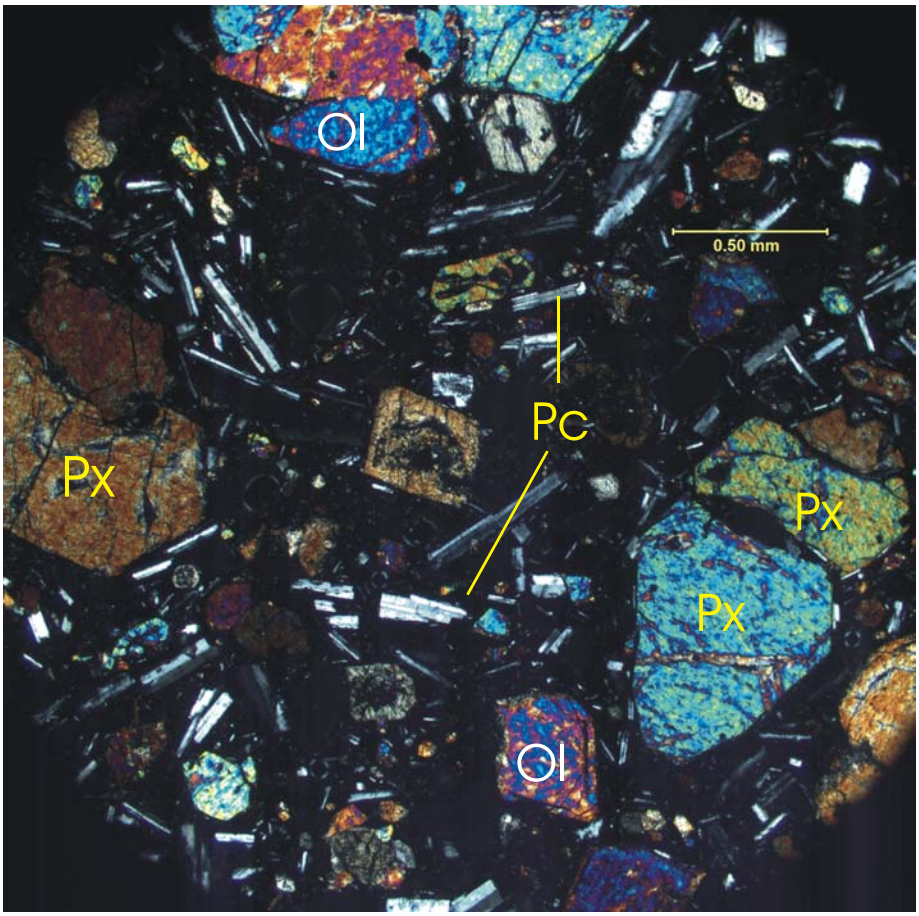

Figure 6. Thin section photomicrograph (crossed nicols) showing a Crater Mountain sample. Px = pyroxene, Pc = plagioclase, Ol = olivine

Red Mountain basalts are similar to those of Crater Mountain. They contain abundant phenocrysts of olivine and plagioclase and a few phenocrysts of resorbed orthopyrox-

ene. Orthopyroxene grains were occasionally rimmed and veined by clinopyroxene. Darrow (1972) described similar rocks in his original study of the Big Pine field. He also noted the presence of scattered grains of nepheline, however, this could not be confirmed in thin section.

The basalts from the flows southeast of Tinemaha Reservoir also contained phenocrysts exceeding 1mm in long dimension. The phenocrysts found in these flows were olivine, clinopyroxene, and plagioclase. Many of the plagioclase phenocrysts were zoned (Fig 7). These basalt flows had a large percentage of glomeroporphyritic phenocrysts. The glomeroporphyritic phenocrysts consisted primarily of plagioclase with some pyroxene and olivine crystals. The non-glomeroporphyritic phenocrysts were mainly plagioclase, with minor clinopyroxene and olivine.

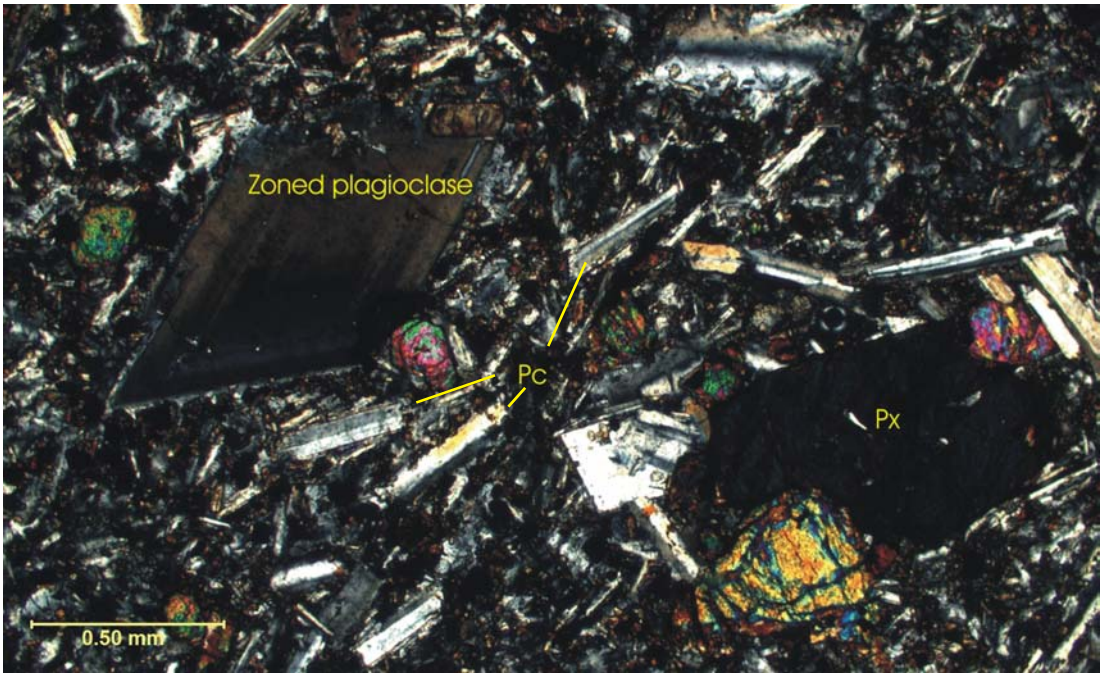

Figure 7. Thin section photomicrograph of basalt southeast of Tinemaha Reservoir. Notice the diamond shaped zoned plagioclase. Pc = plagioclase, px = pyroxene.

The matrix in the Taboose Creek flows was generally very fine-grained and had a slightly different composition when compared to other flows (Fig 8). While it was still primarily plagioclase, the matrix also contained a large percentage of small crystals of olivine and orthopyroxene. Some samples also showed evidence of flow banding with the long axes of plagioclase crystals oriented parallel to flow direction. The phenocrysts in these flows showed

some variation. Some samples had small phenocrysts, most, less than 0.1mm, while others, had slightly larger phenocrysts. In general, the flows from this area had a much smaller percentage of phenocrysts than other flows in the field.

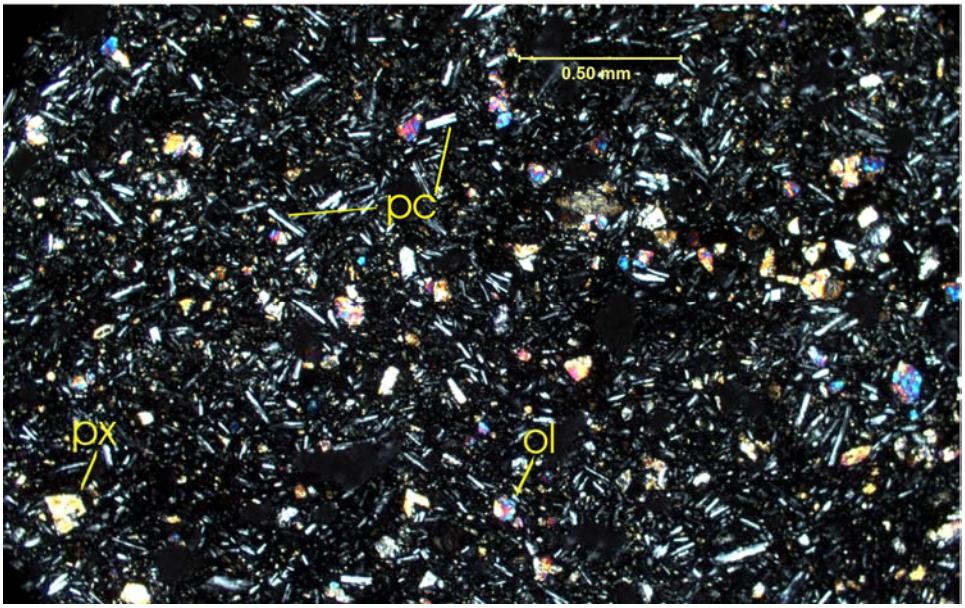

Figure 8. Thin section photomicrograph (crossed nicols). Fine grained basalt from the Taboose Creek area. Pc = plagioclase, ol = olivine, px = pyroxene.

Samples were also collected from a few scattered dikes near Bishop, California. The basalts from the Bishop area are markedly different from those of the Big Pine volcanic field. These basalts have a very fine, glassy, matrix with minor crystalline plagioclase and pyroxene (Fig 9). The sparse phenocrysts exceeded 1mm in long dimension and were occasionally glomeroporphyritic Little or no olivine was present.

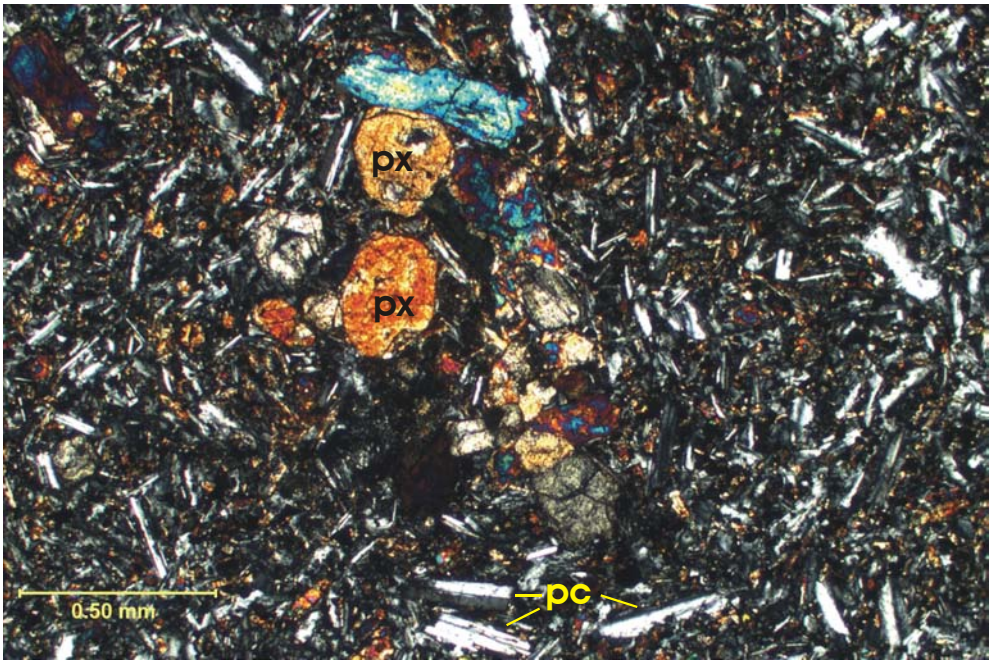

Figure 9. Thin section photomicrograph (crossed nicols). Basalt from Bishop area, notice the lack of olivine.

The general differences in thin section mineralogy (those containing olivine and nepheline and those that do not) have been attributed to crystal fractionation by

other researchers. The differences in proportion and size of phenocrysts may be related to magma residence time in the subsurface. Magmas that rose rapidly to the surface contain only small phenocrysts, lacking evidence of resorption or rounding. Magmas with longer residence times in the crust would contain larger and more numerous phenocrysts with, perhaps some fractionation of the olivine and resorption of both olivine and pyroxene.

Sample Preparation

Upon collection of the hand samples, they were prepared for geochemical analysis. Initially, the samples were crushed using a chipmunk jaw crusher. After crushing, they were poured through a series of sieves (ranging from 200 to 60 microns). The oversized pieces were placed into a steel ball mill and ground for about 30 minutes. When sufficient sample passed through the 60 micron sieve, it was ready to be pressed into a pellet.

To make the pellet, six grams of the sample and 1.2 grams of cellulose binder were added together on an analytical balance. The mixture was placed into a ceramic ball mill, without the ball, and mixed for several minutes. When the mixing was complete, the sample was pelletized using a die and press. An aluminum cup was placed at the bottom of the die and the sample was poured into the die and pressed down with a tamper. The die was then inserted into the press and the pressure pumped to 15 tons. The die stays under 15 tons of pressure for at least one minute. After one minute, the pressure was released and the resulting sample removed. The result was a hard, compact, round, centimeter tall cylindrical-shaped pellet. This process was repeated for each sample.

After the pellets were pressed, they were ready for the x-ray spectrometer (XRF). The XRF analyzed each of the samples and printed the results for major element percentages. The major elements analyzed were *Si*, *Al*, *Ca*, *Mg*, *Fe*, *Mn*, *Na*, *K*, *P*, and *Ti*. Results were reported in weight percent oxide. The major element standards are from the United States Geological Survey. After the XRF had analyzed the major elements, all of the basalts that had over 56% SiO_2 were placed back in the XRF to be analyzed for trace elements in parts per million (ppm). The trace elements analyzed were *Ba*, *Ce*, *Cr*, *La*, *Nd*, *Rb*, *Sr*, *Sc*, *Y*, *Zr*, and *Sm*. The trace element program was developed by Dr. David Jessey at Cal Poly-Pomona.

The resultant analyses were entered into IgPet 2001 to make the various, different petrographic diagrams. This program is capable of producing a wide variety of diagrams, however, only the diagrams that best represented the Big Pine volcanic field data were utilized. These diagrams appear in the Geochemistry section which discusses the geochemistry of the Big Pine volcanic field and compares it to other Owens Valley and Mojave basalt fields.

Geochemistry

Figure 10 summarizes the compositional range for basalts from the Big Pine volcanic field. In general, Big Pine basalts overlap the boundary between subalkaline rocks (basalt and basaltic andesite) and alkaline basalts (trachybasalt and basaltic trachyandesite). Normally, a basalt volcanic field does not straddle the alkaline-subalkaline boundary since this represents a thermal divide. The divide does not permit alkaline magma to produce a subalkaline magma through fractional crystallization (see following section Discussion and Conclusions). Four samples from the Bishop area have been included (stars); they plot predominately in the trachy-basalt field with one plotting in the basalt field.

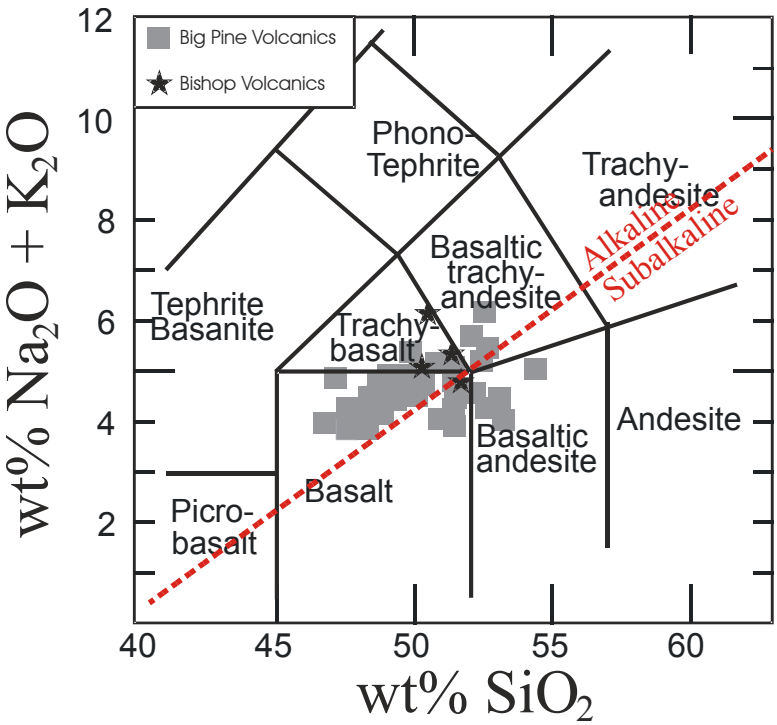

Figure 10. LeBas Diagram showing compositional range of Big Pine and Bishop basalt samples.

The basalt tetrahedron, shown in figure 11, consists of three CIPW normative ternary diagrams that have been merged together. It plots each sample in one of three categories; alkali basalt, olivine tholeiite or tholeiite. The alkali basalt has nepheline (ne),

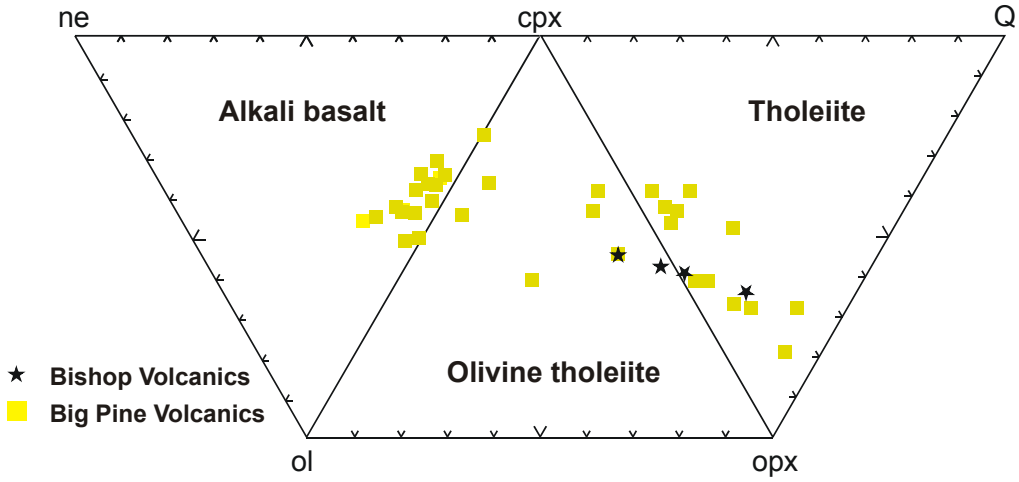

Figure 11. Basalt tetrahedron showing composition of Big Pine and Bishop basalt samples.

clinopyroxene (cpx), and olivine (ol) at the apices of the ternary. The olivine tholeiite ternary is defined by cpx, ol, and orthopyroxene (opx). Tholeiitic basalt has cpx, opx and quartz (Q) at the apices of the triangle. The Big Pine volcanic field is unusual in that it plots across all three triangles. Half of the samples plot in the alkali basalt triangle, a few plot in the olivine tholeiite triangle and the others plot in the tholeiitic ternary. The Bishop samples plot on the line between the olivine tholeiite and tholeiite fields.

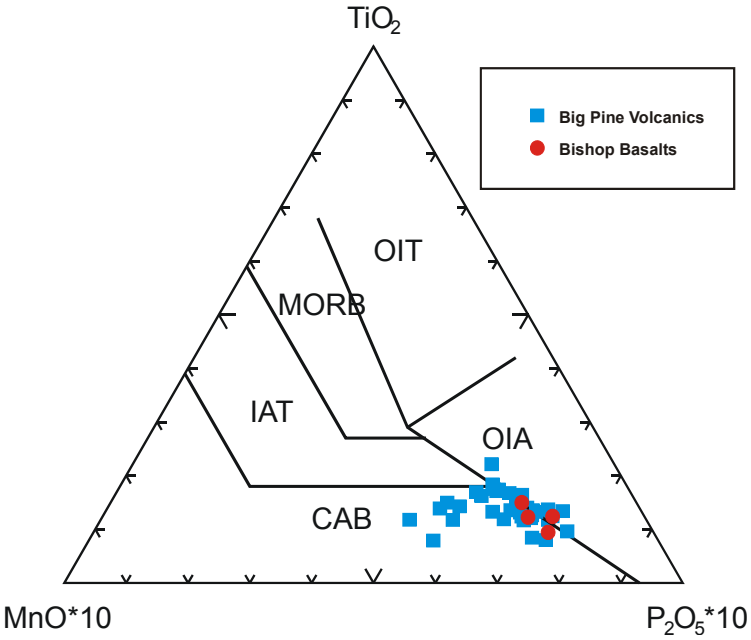

Figure 12. Mullen Diagram showing Big Pine and Bishop volcan-

Mullen and Pearce proposed a series of diagrams whose purpose was to determine tectonic setting. Two of these diagrams are presented herein. The Mullen diagram in Figure 12, plots TiO_2 vs. MnO*10 vs. P_2O_5*10. This diagram shows that the basalts from the Big Pine Volcanic field are all continental arc basalts or ocean island arc basalts. The Bishop samples are directly on the line between the continental arc basalts and the ocean island arc basalts.

The Pearce diagram (Fig. 13) plots MgO vs. FeO* (FeO + Fe_2O_3) vs. Al_2O_3. The Big Pine volcanic field plots from Ocean Ridge to Orogenic. It is not clear exactly what constitutes an orogenic basalt. Presumably Pearce meant orogenic basalts to be the equivalent of Mullen's Continent-

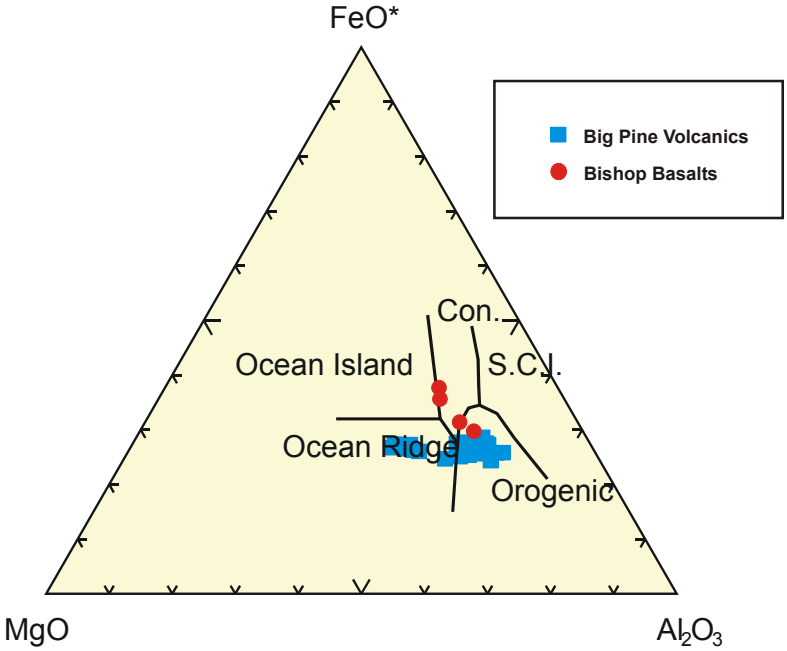

Figure 13. Pearce Diagram showing Big Pine and Bishop volcanics

tal Arc. If this is the case, then the two diagrams display some capability in that they both suggest that some of the Big Pine samples are of continental arc affinity. They differ in that one suggests that some basalts are MORBs and the other that they are OIBs. Such diagrams have to be taken with a degree of skepticism. The actual tectonic setting of the Big Pine basalts is uncertain, but it is unlikely there is any relationship to a continental arc. Even a relationship to MORBs or OIBs is problematic.

The spider diagram (Fig. 14) compares trace element data. This diagram plots *Ba*, *Rb*, *K*, *La*, *Ce*, *Sr*, *Nd*, *P*, *Sm*, *Zr*, and *Y* versus a chrondrite standard. Only the averages for the Bishop area and Big Pine volcanic field are shown. In general, all trace elements are enriched relative to the standard. Although the number of Bishop samples is limited, some speculations can still be made. The Bishop area has higher potassium levels than Big Pine, as well as higher phosphorus levels. Big Pine has higher samarium levels. All of the other trace elements appear to be relatively equal including strontium. The real value of spider diagrams is in their use for comparison of trace element data across various volcanic fields as will be attempted below.

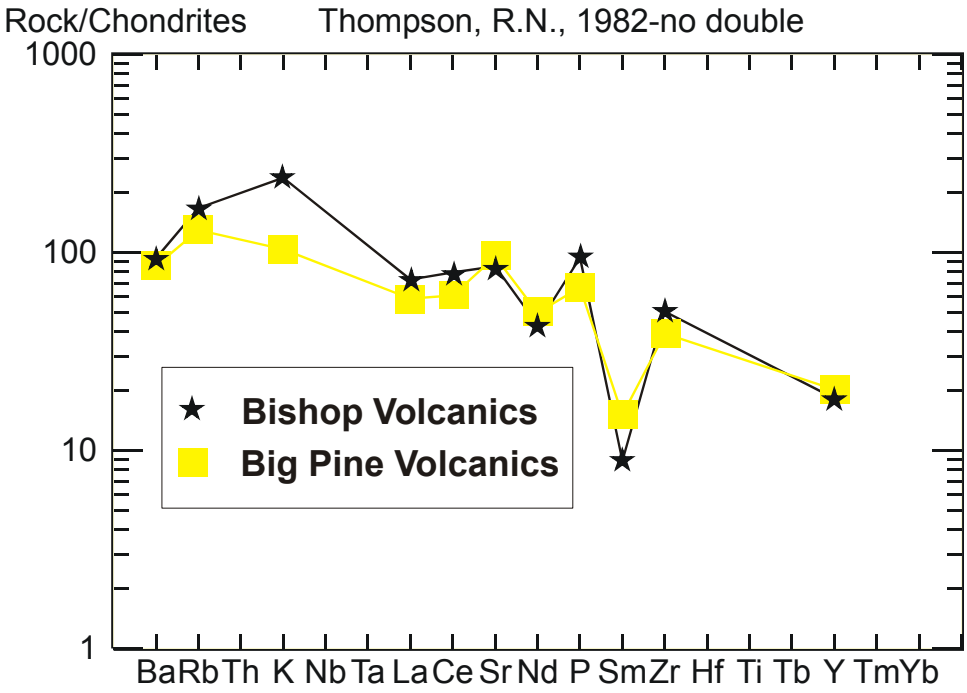

Figure 14. Chrondrite spider diagram showing trace elements for the Bishop and Big Pine basalts.

Figure 15 (LeBas) compares the Big Pine volcanic field to other Owens Valley and Mojave basaltic fields for which data are available. The most noticeable trend was stated previously. The Big Pine field straddles the "normal" basalt-basaltic andesite fields and trachybasalt-basaltic trachyandesite fields. In contrast the Ricardo volcanics lie wholly within the subalkaine basalt and basaltic andesite fields and basalts from the Cima and Coso fields lie within the

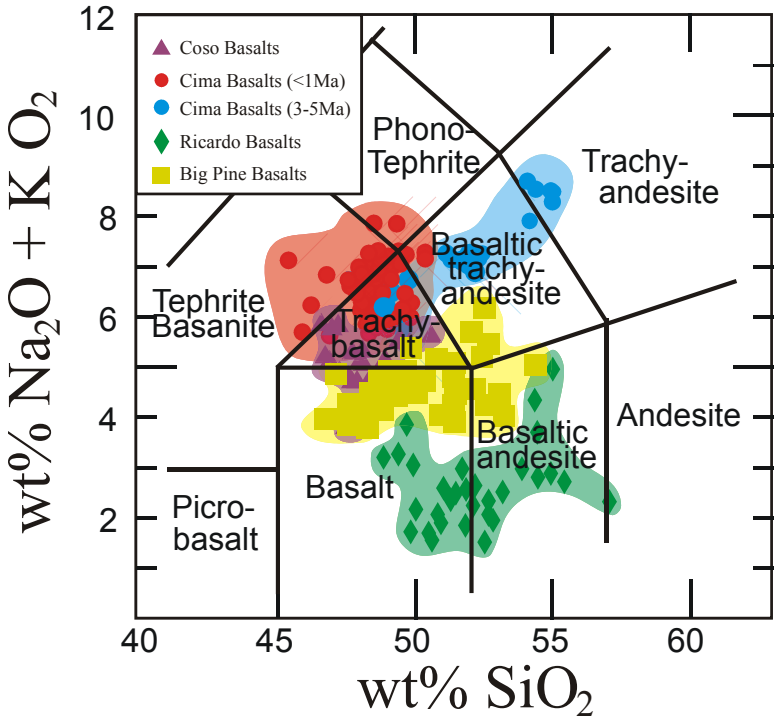

Figure 15. LeBas Diagram showing compositional range of Coso, older and younger Cima, Ricardo and Big Pine volcanic fields. (Coso data from Groves, 1995; Ricardo data from Anderson, 2005)

alkaline trachybasalt and basaltic trachyandesite fields. Therefore, these basalt fields differ dramatically in composition from the Big Pine field.

The anomalous character of the Big Pine field is even more apparent in a basalt tetrahedron (Fig. 16). As in the LeBas Diagram, the Big Pine volcanics plot across all rock types. Half of the samples plot on the alkali basalt side, many others on the tholeiite side; a small number are olivine tholeiites. In comparison, Ricardo volcanics plot in the tholeiite field and Coso and Cima volcanics plot entirely within the alkali basalt field of the tetrahedron. This reinforces the geochemical difference of the Big Pine volcanics, and the broad compositional spectrum; markedly unlike that of any other Owens Valley/Mojave field.

A spider diagram (Fig. 17) and Table 1 display the trace element data for several vol-

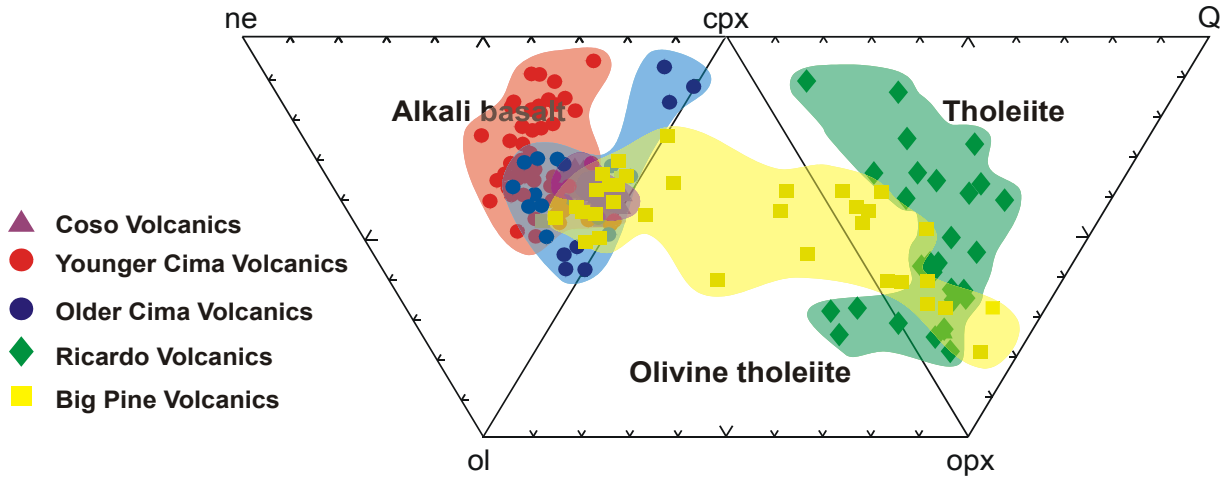

Figure 16. Basalt tetrahedron plotting composition of Coso, younger and older Cima, Ricardo and Big Pine Volcanic fields. Data from same sources as Figure 15.

canic fields. The Big Pine field contains higher concentrations of strontium than any other field, a fact noted in 1972 by Darrow. While cesium and neodymium values are slightly higher than elsewhere, the difference is small.

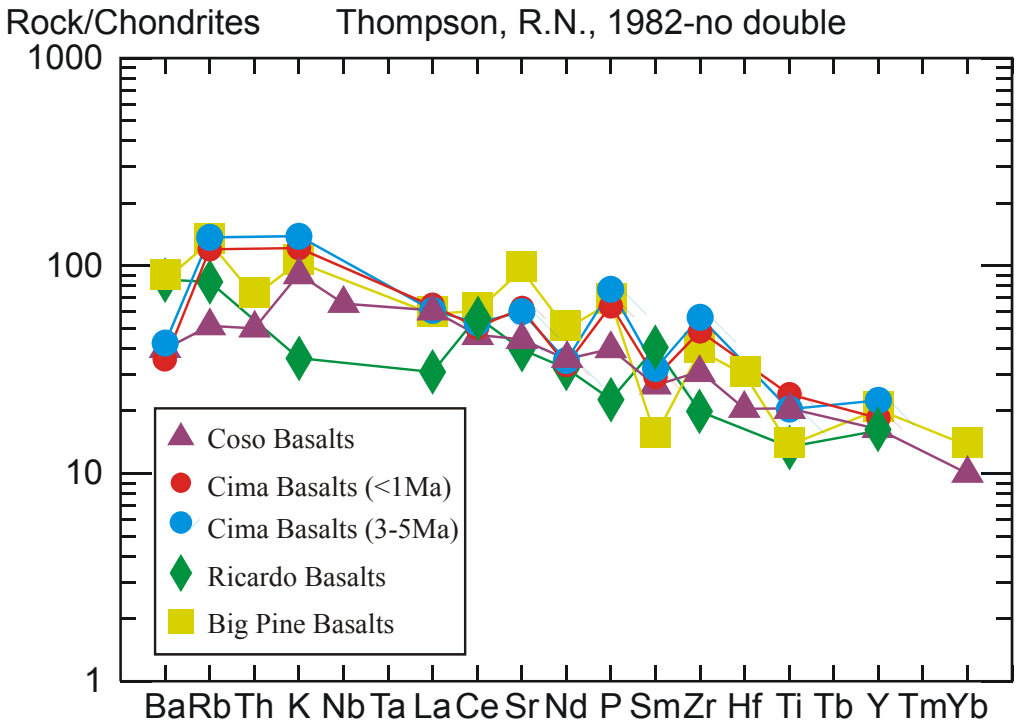

Figure 17. Spider Diagram showing average trace element data for Coso, older and younger Cima, Ricardo and Big Pine Volcanic Fields.

For all other elements there is considerable overlap with other Owens Valley/Mojave fields. Barium is anomalously high for basaltic rocks, but this is a characteristic common to all southern California basalt fields.

Table 2 adopts a different approach. For this table, I averaged those basalts that fall in

Element	*Big Pine*	*Ricardo*	*Coso*	*Older Cima*	*Younger Cima*
Rb	46	29.3	18	48	42
Ba	591	592	275	293	243
Sr	1125	467	522	709	731
Cr	285	248	68	6	82
Zr	267	136	212	387	331
Sc	14	12	24	19	8
La	19	10.1	20	20	21
Ce	53	49.2	40.3	46	44
Nd	31	20.2	22.4	22	21
Sm	5.9	6.5	5.4	8.2	3.1
Y	40.6	32.2	32.7	45	37

Table 1. Trace element (ppm) table comparing Big Pine, Ricardo, Coso, and older and younger Cima fields. Data source as for Figure 15.

the alkali basalt field and tholeiitic basalt fields of the basalt tetrahedron. Some interesting trends can be seen. Alkali basalts contain significantly greater concentrations of strontium, chromium, neodymium and scandium. The former three elements are characteristic of a mantle source. The scandium anomaly may represent analytical error. In contrast, rubidium and to a lesser extent barium and yttrium concentrations are higher in tholeiitic basalts. Rubidium is associated with crustal rocks and the higher content in tholeiites indicates possible crustal contamination. The higher barium values may also represent crustal contamination. The continental crust throughout the California desert has long been known to contain anomalous concentrations of barium and volcanic rocks that represent partial melts of continental crust or that have assimilated continental crust have often been shown to contain elevated barium contents. Reasons for the slightly higher yttrium values are uncertain.

	Rb	Ba	Sr	Cr	Zr	Sc	La	Ce	Nd	Sm	Y
Alkali Basalt	37	573	1248	438	262	18	20	52	43	3	37
Tholeiitic Basalt	54	591	981	143	270	9	18	53	22	4	44

Table 2. Table comparing trace element data (ppm) for alkali and tholeiitic basalts in the Big Pine volcanic field.

Bierman et al., (1991) were the first to suggest that temporal variations existed for the Big Pine field. They indicated that earlier basalts were more alkaline and later basalts less so. They offered no data to support this statement. Blondes (2005) undertook a detailed study of a single cinder cone. Her research showed that older rocks were alkaline while younger rocks were tholeiitic. She concluded there was a distinct temporal trend from alkaline to subalkaline rocks.

I examined my samples to determine if the temporal trend reported by Bierman et al., could be substantiated. Unfortunately, this proved to be more difficult than anticipated. First there is some uncertainty about the age dates reported for the Big Pine field. For instance, Gillespie (1982) reports an *Ar/Ar* age for Crater Mountain of 290 ka, but Stone, et al., (1993) report a *He* exposure date of 110 ka for Crater Mountain. In both cases these ages were derived from very early attempts to use the *Ar/Ar* method and *He* exposure ages. Thus, there may be significant experimental error. Complicating the problem was uncertainty about the actual flows that were sampled. Neither paper was designed to be a definitive study of the volcanic field and hence the authors did not provide detailed sample locations. Therefore, I had to guess about which of my samples corresponded to the reported ages.

With these complications in mind, the oldest rocks sampled would appear to be flows to the east of highway 395 near Tinemaha Reservoir. These were, with one exception, alkaline basalts Samples from the vicinity of Crater Mountain (290 ka, using the more reliable *Ar/Ar* age date) are generally tholeiitic basalts (see Appendix), as are those from Red Mountain (240 ka). The youngest flows sampled are from the vicinity of Taboose Creek. Ages for these flows are controversial, but are generally thought to be around 25 ka (Taylor, 2002) The Taboose flows are a mixture of both alkaline and tholeiitic basalts. Using a certain degree of imagination a case could be made for older alkaline rocks and slightly younger tholeiites. However, it should be stressed that any temporal relationships are extremely tenuous and examples of "younger" alkaline basalts are present (as for example Taboose Creek). Nonetheless, my research does seem to provide some support for Bierman et al., (1991). Or perhaps it is best stated that it does not contradict their hypothesis. The implications of this alkaline --> subalkaline trend will be discussed below.

Discussion

As seen in the Geochemistry section, the Big Pine volcanic field differs from other fields. It has a compositional range straddling four different fields while the Ricardo only straddles two different fields. On the basalt tetrahedron (Figure 16), Ricardo plots almost completely in the tholeiite basalt field, while Big Pine encompass compositions from tholeiitic to alkali basalt. At the other end of the spectrum are the Cima and Coso fields. These fields are higher in $Na_2O + K_2O$ than Big Pine which brings them almost completely out of the basalt range in Figure 15. They are also completely in the alkali basalt field on the basalt tetrahedron (Fig. 16).

Also as seen from the spider diagram (Fig. 18) and Table 1, Big Pine varies from other volcanic fields in terms of some trace element data. The Big Pine field has a much higher level of strontium than any of the other fields. The levels of neodymium and cesium are also higher. The levels of rubidium for Big Pine basalts are close to those of Cima, but much higher than elsewhere. The Big Pine and Ricardo volcanic fields are similar in their amounts of barium and chromium and much higher than Coso, and the older and younger Cima fields. Clearly, the Big Pine field appears to be unique; its genetic history is unlike that of other Owens Valley/Mojave basalt fields. The reasons for this compositional variation will be discussed in this section.

Dilek, et.al., (2002) suggested the distinct geochemistry of the Big Pine volcanics indicated that they originated from separate parental magmas. This necessitates a difference in source area. They offered no suggestion on how or why this source area would differ. While difference in source area would undoubtedly generate basalts of different composition, the relative youth of the Big Pine field argues against such a possibility. Gillespie (1982) undertook a comprehensive geochronologic study of the Big Pine volcanic field. He acknowledged the possibility of basalts as old as 2 Ma, however, none of his dated flows were older than 1.2 Ma. This is a short span of geologic time for emplacement of the Big Pine field and it seems unlikely that source area could change significantly. Baltzer and Jessey (2006) propose differences in source area for older and younger Cima basalts, but their compositional variation is far smaller than that of Big Pine, and the Cima basalts were emplaced over of span of 5+ million years. Furthermore, while differences in source area might account for variation in basalt chemistry, it seems likely that variation would result in clustering of data. We should see two

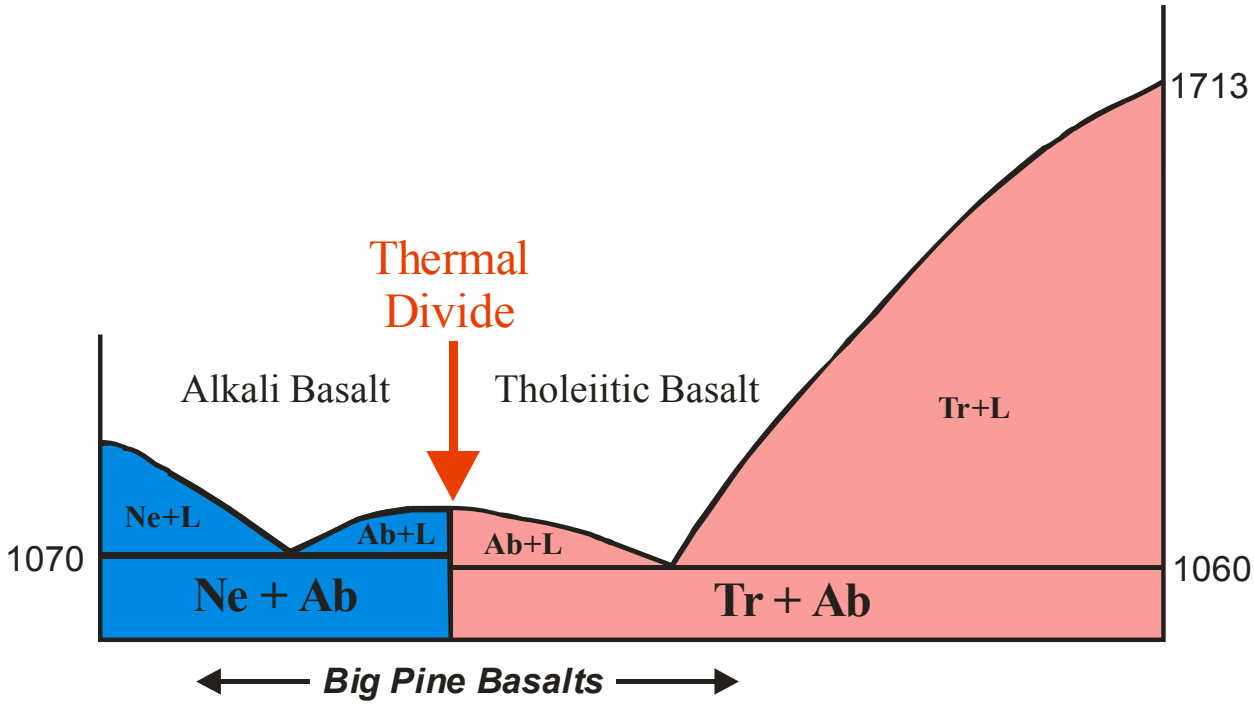

Figure 19. Thermal divide between alkali basalts and tholeiitic basalts. Shows the compositional range of the Big Pine volcanic field (adapted from Winter 2001)

distinct basalt types reflecting the different source areas. This does not explain the spectrum of compositions for the Big Pine field. Not only do we see tholeiitic basalts and alkali basalts, but also some samples which are intermediate, olivine basalts. How would differences in source area account for the compositional spectrum? It seems more likely that one basalt type evolved into the other over time and they share a common source area.

The simplest mechanism for generating tholeiitic magmas from alkaline magmas is through the process of fractional crystallization. Darrow (1972) was the first to suggest this possibility for the Big Pine field, although he regarded it as unlikely. Figure 19 (shown above) illustrates the problem. At low pressure a thermal divide separates ne normative magmas from those that are Q normative. Think of the magma as a rock sitting at the summit of a mountain; it can role down one side or the other, but not both. Thus, a magma can evolve from saturated (olivine basalt) to over saturated (tholeiite) or saturated to undersaturated (alkali basalt), but at low pressure it cannot evolve from undersaturated to oversaturated; the thermal divide prohibits this possibility. Of course, the caveat here is low pressure. At pressures greater than about 1.5 Gpa the thermal divide disappears. This corresponds to a depth of approximately 50 kilome-

ters. Therefore, it would be possible to fractionate a magma if it could be stabilized at depths of 50 kilometers or greater. More recent research allows us to examine this possibility. COCORP seismic studies from the 1980's revealed that the crust beneath this portion of the Owens Valley is roughly 40-45 kilometers thick. Wang et al., (2002) were able to determine the depth of melting of basalts across the Sierra Nevada and Mojave. One of the studied fields was Big Pine (Fig. 20). The calculated melting depth was 40 to 50 kilometers. This is just at the depth/ pressure limit for effective fractionation. Remember, however, that for fractionation to occur, rising magma must also be stabilized. While we might melt at 50 kilometers, the magma would must likely rise to the crust-mantle boundary before ponding. This would represent a depth of 40-45 kilometers, too shallow to allow fractionation from alkaline magmas to tholeiitic magma to occur. Thus, fractionation is not an important process for the Big Pine field. This does not imply, however, that no fractionation occurred. It seems unlikely that any basaltic magma that

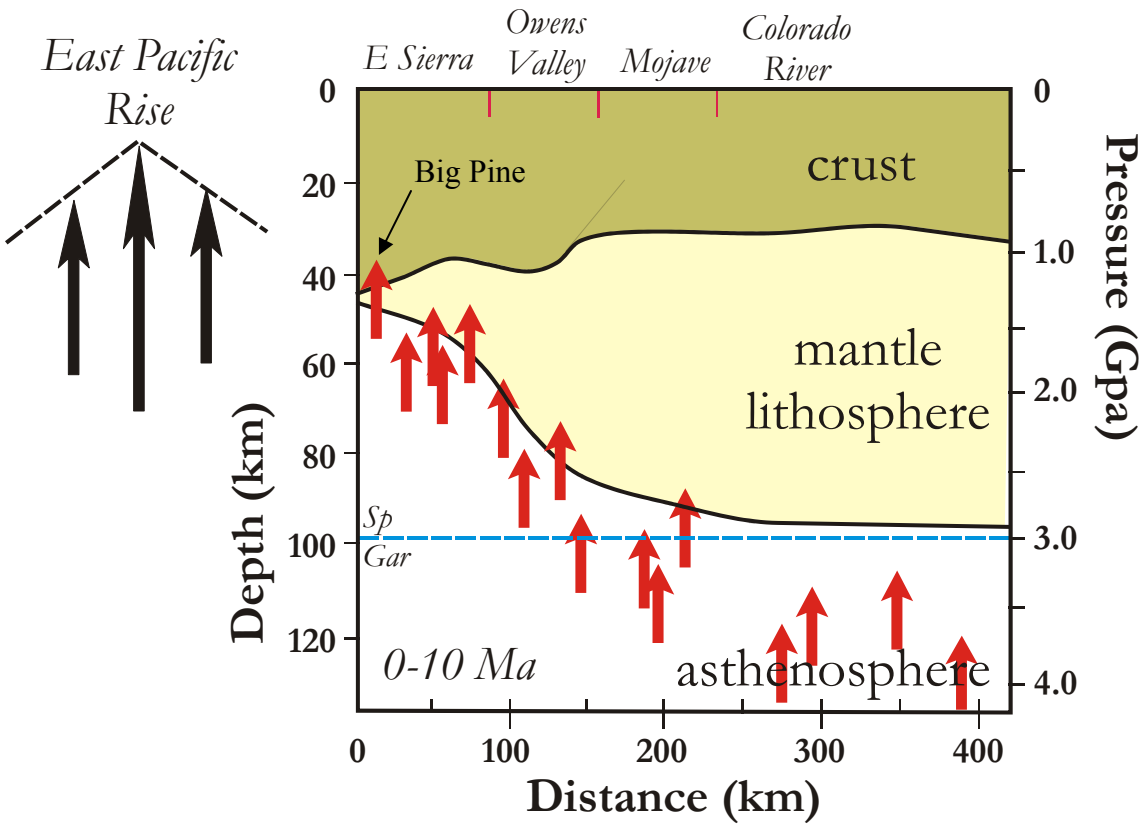

Figure 20. Melting profile across the western Basin and Range. Arrows represent the calculated melting column for each field. (Highly modified from Wang, et al., 2002)

spent time residing at depth would not fractionate at least some of the early-formed, denser, olivine crystals. Hence, fractionation may account for some mineralogic variation, but it was not an effective mechanism for the larger Big Pine basalt compositional spectrum.

Assimilation is another mechanism that can alter magma composition. Previous researchers have generally overlooked or discounted this mechanism. This may be largely because research in the Big Pine field has centered on characterizing the mantle beneath the northern Owens Valley. If the researchers acknowledged crustal contamination in their samples then conclusions on the nature of the mantle would be problematic. Is crustal assimilation a viable alternative?

The bedrock beneath the Owens Valley is generally though to represent portions of the Sierra Nevada batholith down-dropped along dip-slip and oblique-slip faults. While bits and pieces of roof pendant Paleozoic sedimentary rocks have been mapped in the Poverty Hills and southward in the Owens Valley, it is believed that much of this sedimentary cover had been stripped off before Late Cenozoic dip-slip fault movement occurred. Hence, the bedrock is largely Mesozoic granitoid.

If a mantle derived basaltic magma were generated, it would buoyantly rise into the overlying crust. As the liquidus temperature of a basaltic magma (900-1200°C) is well above the melting temperature of a granite (650-800°C) it seems likely that assimilation could occur. Of course, for this to happen the magma assent must be impeded. This would happen at depth because the density of the rising basaltic magma would at some point be equivalent to that of a granite and it would become gravitationally stable. At this point pooling would occur and granitic host rock would be assimilated. Also, some fractionation of olivine might accompany the assimilation. This could dramatically alter the magma composition. So it is possible to generate a tholeiitic magma from an alkaline magma through assimilation, and perhaps some fractionation.

But how does this account for the compositional spectrum of Big Pine basalts? To answer that we need to look at the structural setting of the field. All flows and scoria cones in the Big Pine field lie along active faults. Indeed, Big Pine is the most structurally controlled field in the Owens Valley/Mojave. Assuming that Big Pine basalts become gravitationally stable at depth, the only mechanism to allow the magmas to reach the surface would be an open conduit. For this reason, the basaltic magmas can reach the surface only when an earthquake breaches an

active fault. Then the magma would be free to rise along the dilated fault plane to the surface. The compositional spectrum reflects residence time. Basaltic magmas that rose quickly from the lower crust along a fault would be largely uncontaminated and yield alkali basalts. Those that were trapped at depth would evolve until an open conduit presented itself and rise to the surface generating olivine basalts and tholeiitic basalts.

While this is an attractive theory, is there evidence to support it? Figure 21 is ε-neodymium isotope diagram. This type of diagram often requires extensive explanation. Note that the Big Pine volcanic field is enriched in ^{87}Sr relative to the mantle array and contains a lower concentration of radiogenic neodymium, at least relative to *Bulk Earth*. This is significant. If a basalt is generated from a partial melt of the mantle and has not interacted with crustal rocks it should plot wholly within the Mantle Array. The Coso and Cima fields are examples of such an evolutionary path; they plot on the mantle array. Big Pine, however, lies

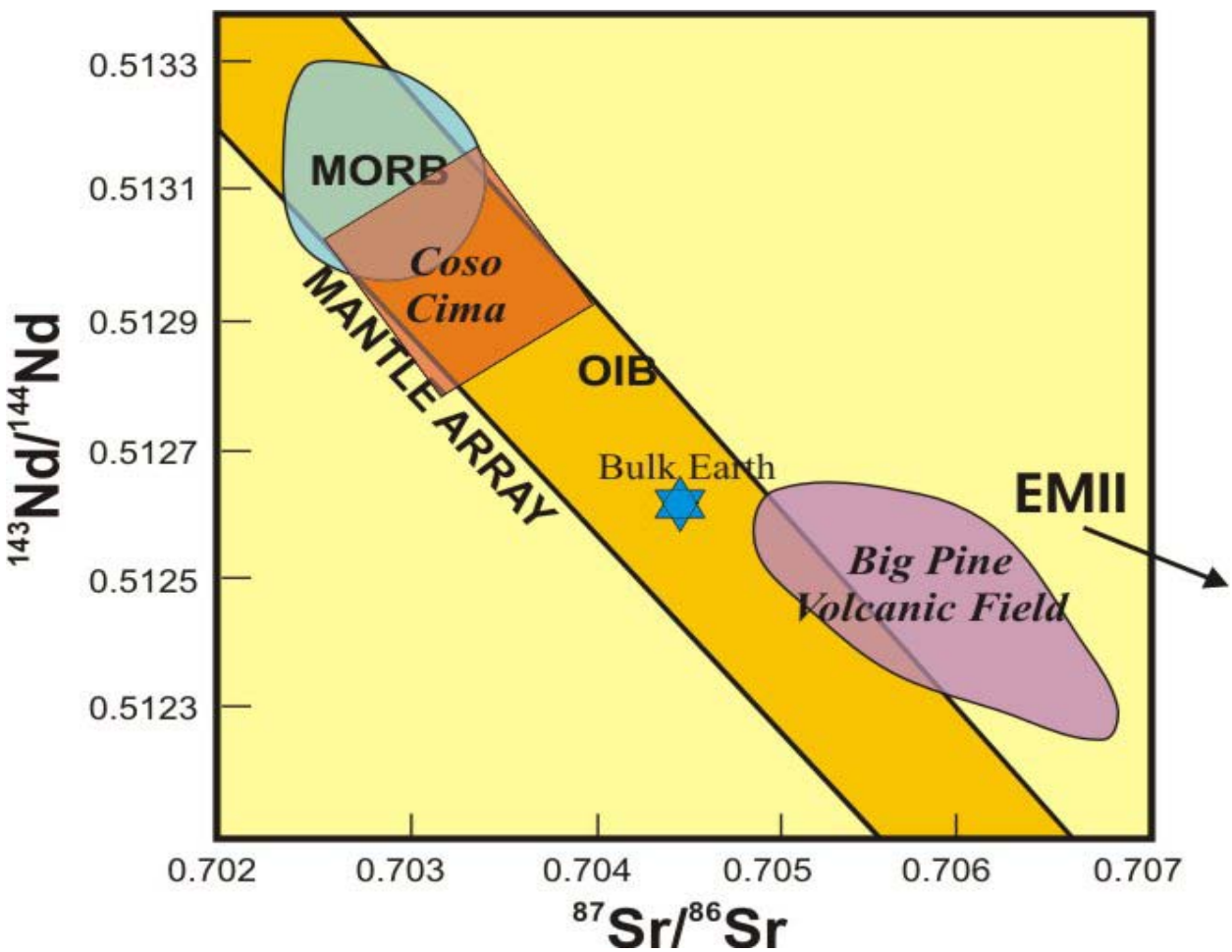

Figure 21. ε-neodymium diagram comparing the mantle array to the Big Pine volcanic field, the Coso and Cima fields, and a MORB basalt (Sone data from Waits, 1995).

largely outside the Mantle Array. There are a plethora of hypothetical reservoirs that have been proposed to account for basalts which lie outside the Mantle Array. In the case of Big Pine, EMII is the only good fit as a reservoir. For the uninitiated, EMII represents average silicic crust. Thus to generate the isotopic ratios seen for Big Pine would necessitate mixing of mantle and crust, or more reasonably assimilation of crustal material.

Trace element data also supports assimilation. Table 2 broke down Big Pine basalts into alkali and tholeiitic basalts. The latter were significantly enriched in rubidium and less so in barium and zirconium. Rubidium, barium and zirconium are incompatible elements and would be expected to be enriched in granitoidal rocks. Crustal assimilation would then enrich the basaltic magmas in these elements. In contrast, chromium, strontium and neodymium are enriched in alkali basalts. Chromium substitutes for iron in olivine and *Sr* and *Nd* for calcium in plagioclase. These could have been fractionated out during ponding of the magmas.

My model envisions the following sequence of events:

- Basaltic magmas generated in mantle rise into the overlying crust. (The source/tectonic setting for these magmas remains enigmatic.)
- Some magmas rise directly to the surface if an open channelway is present (alkali basalt).
- Other magmas are pooled at depth due to gravitational stability. These assimilate granitoidal rocks, and perhaps undergo slight fractionation yielding the olivine basalts and tholeiitic basalts.
- The latter magmas reach the surface when earthquakes breach existing faults re-opening clogged channelways.

Bierman et al, (1991) were the first to suggest a temporal relationship for Big Pine basalts. They proposed early basalts were alkaline and later basalts subalkaline. Dilek et al., (2002) also suggested a temporal relationship with older basalts to the south and west and younger flows to the north and west. Blondes (2005) demonstrated that temporal relationships also existed within individual flows.

As stated previously (Geochemistry) my research tends to provide some credence to this hypothesis, although it is tenuous at best. Older flows around Tinamaha Reservoir are generally alkaline while younger flows at Crater and Red Mountains are tholeiitic. Unfortunately,

there is significant uncertainty and overlap with some of the youngest flows along Taboose Creek being a mixture of both rock types. Thus, it is perhaps safest to say that a temporal relationship may exist with younger flows being predominantly tholeiitic, but more geochemistry and geochronology needs to be done.

This, in fact, presents an interesting question. If tholeiitic basalts are generated only when magmas undergo substantial residence time in the crust, and this happens only when a channelway is not available; does it follow that a longer recurrence interval between major earthquakes would favor tholeiites? If so, does this imply that the rate of seismicity has decreased within the northern Owens Valley over the past one million years?

References Cited

Anderson, Cami Jo, 2005, A Geochemical and Petrographic Analysis of the Basalts of the Ricardo Formation Southern El Paso Mountains, CA, unpublished Senior Thesis, Cal Poly-Pomona, 37p.

Anderson, Cami Jo, and Jessey, D.R., 2005, Geochemical analysis of the Ricardo Volcanics, southern El Paso Mountains, CA, Geological Society of America Cordilleran Section Abstract with Programs Volume, San Jose, CA.

Baltzer, Suzanne, Jessey, D.R., 2006, Late Cenozoic volcanism near Baker, California, Southern California Academy of Sciences Symposium, Pepperdine University, Malibu, CA

Bierman, Paul R.; Clark, Douglas; Gillespie, Alan; Hanan, Barry B., editor; Whipple, Kelin X. 1991, Quaternary geomorphology and geochronology of Owens Valley, California; Geological Society of America field trip. Geological excursions in Southern California and Mexico, Walawender, Michael J., editor. San Diego, CA: San Diego State Univ., p. 199-223.

Bishop, Kim M. 2000, Large-scale mass wasting deposits of the Owens Valley, southeastern California. Field Trip Guide, Eastern Sierra Geological Society, 32 p.

Blondes, M.S., Reiners, P.W., Kayzar, T.M., Ducea, M.N., and Chesley, J.,, 2005, Using temporal-compositional trends in single eruption sequences of primitive basalts to observe systematic time-dependent mantle source variation: an example form the Big Pine volcanic field, California.

Darrow, Arthur, 1972, Origin of the basalts of the Big Pine volcanic field, California, unpublished Master's Thesis, UCSB.

Dilek, Y., Robinson, P.T., and Bondre, N., 2002, Tectonic Setting of the Big Pine Volcanic Field. Eastern California, Eos Trans. AGU, 83(47), Fall Meet. Suppl., Abstract V12B-1435.

Gillespie, A.R., 1982, Quaternary glaciation and tectonism in the southeastern Sierra Nevada, Inyo County, California, Ph.D. dissertation, California Institute of Technology.

Groves, Kristelle, 1996, Geochemical and isotope analysis of Pleistocene basalts from the southern Coso volcanic field, California, unpublished Master's Thesis, UNC-Chapel Hill, 84 p.

LeBas, M.J., 1986, A chemical classification of volcanic rocks based on the total alkali silica diagram, J. Petrol. 27: 745-750.

Mullen, E.D., 1983, MnO/TiO2/P2O5: A minor element discriminant for basaltic rocks of oceanic environments and its implications for petrogenesis, E.P.S.L., 62: 53-62.

Pearce, J.A., Harris, B.W., and Tindle, A.G., 1984, Trace element discrimination diagrams for the tectonic interpretation of granitic rocks, J. Petrol. 25: 956-983.

Ringwood, A.E., 1976, Composition and petrology of the Earth's mantle, McGraw Hill Book Company, New York, NY, 618 p.

Ross, Donald C., 1965, Geology of the Independence Quadrangle, Inyo County, California. Geological Survey Bulletin 1181-0. U.S. Government Printing Office, Washington.

Sharp, Robert P., and Glazner, A.F., 1997, Geology Underfoot in Death Valley and Owens Valley, Mountain Press Publishing Company, p. 1-201.

Stone, J.O., Friedrichsen, H., Hammerschmidt, K., Hilton, D., 1993. Cosmogenic He-3 ages of basalts at Big Pine, California, constraints on uplift across the Owens Valley fault zone. Eos, Transactions, American Geophysical Union, vol. 74, no. 43 Suppl., p. 609.

Taylor, T.R., 2002, Origin and structure of the Poverty Hills, Owens Valley fault zone, Owens Valley, California, unpublished Master's Thesis, Miami University.

Waits, J.R., 1995, Geochemical and isotope study of peridotite-bearing lavas in eastern California, unpublished Master's Thesis, UNC-Chapel Hill, p. 60.

Wang, K., Plank, T., Walker, J.D., and Smith, E.I., 2002, A mantle melting profile across the Basin and Range, SW USA, pp ECV 5-1-19.

Winter, J.D., 2001, An Introduction to Igneous and Metamorphic Petrology, Prentice Hall, p. 699.

Appendix A
Major Element Table

Sample	Flow	SiO_2	TiO_2	Al_2O_3	Fe_2O_3	MnO	MgO	CaO	Na_2O	K_2O	P_2O_5
BS01	Bishop	50.387	2.070	13.527	13.027	0.256	5.888	7.748	1.211	4.967	0.919
BS02	Bishop	51.000	1.569	16.368	10.202	0.186	5.343	8.933	2.814	2.669	0.916
BS04	Bishop	51.450	1.509	15.526	10.818	0.278	5.837	8.637	1.762	2.989	1.194
BS05	Bishop	49.569	1.690	14.257	12.580	0.258	6.301	9.260	1.928	3.210	0.948
TR01	Black Rock Road	47.470	1.379	14.393	10.586	0.213	10.719	10.685	2.376	1.511	0.668
TR02	Black Rock Road	48.076	1.299	14.875	10.226	0.297	9.617	10.555	2.167	1.679	1.209
TR03	Black Rock Road	48.186	1.288	15.721	9.854	0.186	9.473	10.204	2.930	1.446	0.712
TR04	Black Rock Road	47.683	1.325	15.243	9.865	0.223	9.624	11.048	2.703	1.518	0.768
TR05	Tinemaha	50.095	1.407	16.023	8.950	0.182	6.071	11.816	3.008	1.733	0.716
TR06	Tinemaha	51.075	1.435	17.154	8.651	0.156	5.453	9.515	4.016	1.804	0.740
TR07	Tinemaha	50.680	1.462	16.613	9.121	0.214	5.768	10.168	3.671	1.539	0.765
TR08	Tinemaha	49.929	1.403	17.312	9.484	0.272	6.326	9.839	3.174	1.493	0.769
TR09	Tinemaha	48.905	1.481	17.407	9.520	0.214	5.937	11.002	3.247	1.546	0.743
TR10	Tinemaha	48.467	1.339	16.348	8.836	0.205	7.779	12.021	2.665	1.572	0.768
TR11	Tinemaha	51.384	1.428	15.898	8.230	0.208	5.981	10.592	3.428	1.710	1.140
TR12	Tinemaha	51.159	1.403	17.216	9.162	0.334	5.627	9.705	2.675	1.534	1.186
TR13	Crater Mtn	51.414	1.434	18.418	9.867	0.381	5.286	8.304	2.649	1.555	0.691
TR14	Crater Mtn	51.965	1.346	17.300	9.157	0.313	5.883	8.925	3.077	1.512	0.522
TR15	Crater Mtn	53.048	1.306	18.546	8.924	0.426	4.548	8.135	2.761	1.752	0.555
TR16	Crater Mtn	51.409	1.429	17.774	9.706	0.258	5.544	8.888	2.951	1.372	0.669
TR17	Crater Mtn	53.197	1.216	15.943	8.889	0.247	5.696	10.265	2.809	1.255	0.484
TR18	Crater Mtn	52.625	1.255	15.885	8.361	0.185	6.529	10.092	3.045	1.322	0.431
TR19	Crater Mtn	50.924	1.372	17.412	10.147	0.637	5.242	9.183	2.420	1.688	0.975
TR20	Crater Mtn	52.507	1.430	16.924	7.898	0.187	5.045	8.948	3.646	2.546	0.868
TR21	Crater Mtn	46.544	1.408	14.546	10.348	0.182	11.020	11.248	2.581	1.441	0.682
TR22	Red Mtn	52.407	1.443	16.976	8.887	0.157	5.887	8.426	3.301	1.937	0.580
TR23	Red Mtn	52.615	1.485	17.231	8.805	0.140	5.201	8.199	3.567	1.942	0.814
TR24	Red Mtn	51.328	1.618	18.575	9.085	0.145	4.954	8.950	3.250	1.670	0.425
TR25	Red Mtn	54.357	1.345	16.691	8.352	0.173	4.937	8.290	3.298	1.853	0.705
TR26	Taboose Creek	49.578	1.455	17.360	9.478	0.172	5.881	10.786	3.799	1.014	0.476
TR27	Taboose Creek	49.191	1.497	16.599	9.892	0.188	6.838	10.720	3.606	0.949	0.519
TR28	Taboose Creek	48.840	1.566	16.515	9.871	0.191	6.663	11.240	3.633	0.927	0.555
TR29	Taboose Creek	50.917	1.508	17.288	9.422	0.191	5.040	10.982	3.035	1.074	0.542
TR30	Taboose Creek	51.284	1.443	16.693	9.670	0.296	5.565	10.585	2.679	1.258	0.527
TR32	Taboose Creek	49.769	1.507	16.275	9.351	0.179	6.766	9.826	3.451	1.993	0.883
TR33	Taboose Creek	46.934	1.353	15.474	10.317	0.219	10.247	9.835	3.470	1.406	0.744
TR34	Taboose Creek	47.501	1.411	14.980	10.114	0.213	9.918	10.796	2.901	1.443	0.724
TR35	Taboose Creek	48.604	1.507	17.286	10.036	0.190	6.459	10.579	3.702	0.992	0.644
TR36	Taboose Creek	48.576	1.494	18.483	9.768	0.174	5.766	10.981	3.196	0.998	0.564
TR37	Taboose Creek	51.286	1.465	16.861	9.707	0.221	5.534	10.240	3.062	1.090	0.534
BSAVG		50.602	1.710	14.920	11.657	0.245	5.842	8.645	1.929	3.459	0.994
TRAVG		50.555	1.444	16.481	9.578	0.238	6.408	9.821	2.952	1.771	0.745

Appendix 2
Trace Element Table

Sample	Flow	*Rb*	*Ba*	*Sr*	*Cr*	*Zr*	*Sc*	*La*	*Ce*	*Nd*	*Sm*	*Y*
BS01	Bishop	75.17	1175.05	1013.29	86.62	391.93	9.87	24.18	71.46	30.20	0.61	42.24
BS02	Bishop	48.25	981.64	1172.56	232.18	318.69	5.32	24.50	64.50	24.16	0.31	35.43
BS04	Bishop	61.67	1094.02	912.11	309.58	339.46	0.46	21.93	67.51	24.10	2.13	36.44
BS05	Bishop	50.03	1301.91	926.47	452.18	327.52	24.69	25.43	71.74	30.24	4.16	32.65
TR01	Black Rock Road	35.24	640.29	1243.47	847.80	255.03	20.36	20.45	54.45	33.61	3.84	34.19
TR02	Black Rock Road	46.46	727.92	1224.99	778.81	249.47	19.17	28.89	57.07	36.28	3.23	36.29
TR03	Black Rock Road	32.29	655.69	1304.92	753.22	255.93	17.11	23.37	54.15	32.18	3.39	32.66
TR04	Black Rock Road	35.11	697.48	1399.28	790.25	257.01	19.06	23.52	55.14	28.78	3.35	32.86
TR05	Tinemaha	51.18	658.43	1436.76	168.31	293.80	14.84	16.87	55.91	23.37	1.63	41.59
TR06	Tinemaha	44.30	524.42	1106.86	190.03	271.07	2.51	17.69	50.75	20.07	0.76	42.21
TR07	Tinemaha	41.39	622.96	1074.09	205.46	260.17	16.14	17.46	52.08	20.73	2.09	40.61
TR08	Tinemaha	49.77	547.06	1028.95	244.68	271.65	8.24	21.81	51.63	27.74	3.24	43.01
TR09	Tinemaha	47.14	438.63	1005.57	219.15	266.52	10.73	16.87	47.57	23.89	2.55	42.76
TR10	Tinemaha	58.97	424.15	981.57	183.23	272.68	13.00	13.10	47.63	20.83	0.52	43.96
TR11	Tinemaha	50.24	555.04	1097.57	138.14	279.34	9.97	15.90	51.38	13.37	2.54	45.21
TR12	Tinemaha	57.38	627.36	968.28	186.44	275.15	12.14	18.90	54.68	22.78	2.40	47.32
TR13	Crater Mtn	62.15	554.95	794.10	284.67	260.54	6.73	21.50	53.49	30.20	6.71	46.48
TR14	Crater Mtn	54.82	528.27	846.86	289.31	258.85	3.59	16.87	50.42	22.43	4.41	44.07
TR15	Crater Mtn	74.26	647.25	801.40	140.70	295.46	3.70	15.63	54.47	25.66	1.97	50.69
TR16	Crater Mtn	49.45	478.87	823.82	261.25	250.91	8.89	20.57	49.71	23.26	4.37	42.83
TR17	Crater Mtn	48.92	409.39	856.47	144.14	231.29	5.54	15.79	47.36	11.39	1.61	41.20
TR18	Crater Mtn	45.42	398.76	856.05	158.69	236.62	7.60	14.19	45.49	17.29	3.25	41.94
TR19	Crater Mtn	67.68	705.27	811.37	159.66	271.82	7.60	24.46	60.62	30.55	6.82	50.01
TR20	Crater Mtn	65.78	961.56	1556.99	35.47	320.03	6.04	16.56	62.32	27.18	0.24	45.16
TR21	Crater Mtn	27.78	656.79	1637.78	1000.34	258.16	24.90	24.15	55.57	288.89	2.60	31.64
TR22	Red Mtn	58.37	902.81	1164.69	104.89	300.24	4.30	17.92	60.69	19.62	3.42	42.66
TR23	Red Mtn	54.98	698.40	1149.48	65.53	304.13	1.21	18.78	54.56	21.56	2.53	43.73
TR24	Red Mtn	49.88	748.63	1293.65	56.36	311.86	10.62	21.23	55.74	23.96	4.43	42.66
TR25	Red Mtn	59.22	832.04	1129.41	87.27	283.91	6.68	19.64	58.17	19.62	3.41	44.43
TR26	Taboose Creek	26.88	533.04	1054.20	178.61	236.62	23.39	15.59	50.19	17.47	2.42	33.88
TR27	Taboose Creek	29.61	443.94	1007.00	133.95	237.62	26.31	16.56	47.52	25.00	2.89	35.54
TR28	Taboose Creek	27.05	375.11	1049.70	182.77	245.79	22.85	20.10	46.16	22.12	3.25	36.66
TR29	Taboose Creek	38.40	393.44	1082.78	84.17	246.88	15.60	12.99	45.97	24.65	1.57	40.18
TR30	Taboose Creek	50.33	458.70	1009.24	122.20	271.09	30.20	15.55	49.20	20.49	3.10	43.45
TR32	Taboose Creek	49.87	883.37	1683.64	313.85	329.31	11.16	23.14	61.53	29.41	3.71	49.87
TR33	Taboose Creek	31.81	526.62	1422.56	719.32	265.84	16.57	25.27	50.99	30.13	6.27	33.60
TR34	Taboose Creek	32.47	633.50	1311.32	773.63	259.22	16.14	22.90	54.40	30.41	3.04	34.52
TR35	Taboose Creek	22.82	510.13	1071.94	110.36	232.20	27.72	20.88	48.98	21.67	3.96	32.50
TR36	Taboose Creek	23.55	404.99	1095.86	127.12	232.63	23.50	14.23	46.70	18.99	2.22	33.75
TR37	Taboose Creek	37.63	485.19	1123.23	6.41	248.93	17.66	21.81	48.91	22.33	3.01	38.39
BSAVG		58.78	1138.15	1006.11	270.14	344.40	10.08	24.01	68.80	27.18	1.80	36.69
TRAVG		49.30	665.22	1100.15	274.00	278.19	12.30	19.49	54.77	31.80	2.84	41.04